

An invertible generative model for forward and inverse problems

Tristan van Leeuwen^{1,3}, Christoph Brune², and Marcello Carioni²

¹Centrum Wiskunde en Informatica, Amsterdam, The Netherlands

²University of Twente, Enschede, The Netherlands

³Utrecht University, Utrecht, The Netherlands

September 5, 2025

Abstract

We formulate the inverse problem in a Bayesian framework and aim to train a generative model that allows us to simulate (i.e., sample from the likelihood) and do inference (i.e., sample from the posterior). We review the use of triangular normalizing flows for conditional sampling in this context and show how to combine two such triangular maps (an upper and a lower one) in to one invertible mapping that can be used for simulation and inference. We work out several useful properties of this invertible generative model and propose a possible training loss for training the map directly. We illustrate the workings of this new approach to conditional generative modeling numerically on a few stylized examples.

1 Introduction

Inverse problems occur in many applications and are typically formulated in terms of a *forward operator*, $K : \mathbb{R}^n \rightarrow \mathbb{R}^m$, *measurements*, $\mathbf{f} \in \mathbb{R}^m$, and entails finding $\mathbf{u} \in \mathbb{R}^n$ such that $K\mathbf{u} = \mathbf{f}$. This problem is typically ill-posed as an inverse of K does not exist or at best is highly unstable. In some cases, when the problem is only mildly ill-posed, it is possible to derive an explicit expression for a regularized inverse $R \approx K^\dagger$ which can also be efficiently evaluated. A prime example is the filtered back-projection method for CT reconstruction [18, and references therein] or the Wiener filter for image deblurring [16, and references therein]. While computationally very efficient, such explicit constructions typically require fully sampled measurements. Thus, measurements take a long time, but computation is relatively cheap.

There is a growing interest in reducing measurement time, leading to under-sampled data and a failure of these so-called *direct inversion* methods. In those

cases, the inverse problem is posed as a *variational problem*

$$\min_{\mathbf{u} \in \mathbb{R}^n} \mathcal{D}(K\mathbf{u}, \mathbf{f}) + \mathcal{R}(\mathbf{u}), \quad (1)$$

with $\mathcal{D} : \mathbb{R}^m \times \mathbb{R}^m \rightarrow \mathbb{R}_+$ the *data-fidelity* and $\mathcal{R} : \mathbb{R}^n \rightarrow \mathbb{R}^+$ the *regularization term*. This implicitly defines the inverse mapping $R : \mathbb{R}^m \rightarrow \mathbb{R}^n$ and provides a powerful framework for analysis and algorithm design [39]. The resulting optimization problem is often cumbersome to solve, requiring many evaluations of K to converge using some iterative scheme. Thus, we arrive at a situation where measurement time is short but computation time is long.

Data-driven approaches aim at closing the gap in computational efficiency between direct and variational methods by learning a mapping $R : \mathbb{R}^m \rightarrow \mathbb{R}^n$ from example data $\{(\mathbf{u}_i, \mathbf{f}_i)\}_{i=1}^N$ [6]. When the learned inverse can be evaluated efficiently, we can use it for fast inference at the expense of a computationally intensive off-line training phase. Care needs to be taken here with the inherent ill-posedness; if the training data contains samples for which $\|\mathbf{f}_i - \mathbf{f}_j\|/\|\mathbf{u}_i - \mathbf{u}_j\|$ is small, the resulting map R may be highly ill-conditioned. Despite that, notable examples have achieved impressive reconstruction results for a wide range of inverse problems [2, 20, 14, 30, 45, 32].

A different perspective is given by the *Bayesian framework* in which \mathbf{u}, \mathbf{f} are interpreted as realizations of random variables, \mathbf{U}, \mathbf{F} , that follow some underlying distribution [41]. Typically, one formulates a *prior* distribution (defining a probability measure for \mathbf{U}) and a likelihood (defining a conditional probability for \mathbf{F} given $\mathbf{U} = \mathbf{u}$). As per Bayes' rule, this results in a *posterior* distribution, giving a conditional probability measure of \mathbf{U} given $\mathbf{F} = \mathbf{f}$. Well-posedness of the problem (i.e., when does this lead to a well-defined posterior distribution) is for example presented by. In a way, the posterior is the ultimate answer to the inverse problem, as it captures assumptions on the data-generating process and prior information and allows us to give a probabilistic answer. Characterising the posterior in general is difficult, and one often results to either estimating the mode (the MAP estimate) and local variance (i.e., the Fischer information) or drawing samples from it using MCMC techniques. MAP-estimation again results in an optimization problem of the form (1) and the Fischer information involves computing and inverting a matrix of second-order derivatives of the log-posterior. This can be challenging for high-dimensional problems, although matrix-sketching techniques have been developed to push the boundaries of this approach [4]. MCMC-sampling techniques, on the other hand, are a powerful way to more accurately characterize complicated probability distributions, but suffer from the curse of dimensionality. Alleviating this is a very active field of research with many success stories [10]. Still, the computational cost can be forbidding as long burn-in periods may be needed.

Generative models can generate samples from complicated probability distributions efficiently [15, 22, 24, 34], and these have also been applied to uncertainty quantification in inverse problems [1, 35, 36]. The basic gist of these methods is that they are trained in an off-line phase based on training data and are then deployed to generate samples from the corresponding posterior efficiently. Gener-

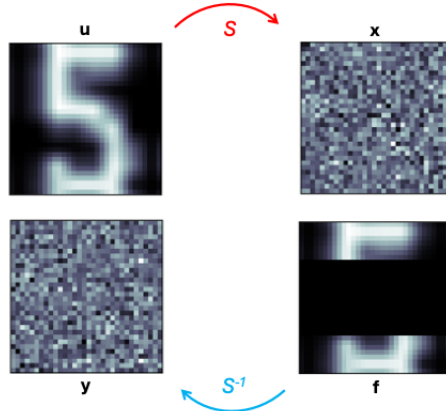


Figure 1: Schematic depiction of the map S for an inpainting problem. In this example, the simulation entails removing part of the digit. The inverse of the map produces an inpainted digit.

ally, this leads to a map $R : \mathbb{R}^{n+m} \rightarrow \mathbb{R}^m$ that will map samples from a reference distribution to samples from the posterior, i.e. $\mathbf{U} = R(\mathbf{X}, \mathbf{f})$ with \mathbf{X} distributed according to a reference distribution over \mathbb{R}^n (i.e., standard normal) will result in \mathbf{U} being distributed according to the posterior conditioned on \mathbf{f} . Similarly, we may train a generative model to sample from the likelihood distribution, yielding a map $S : \mathbb{R}^{n+m} \rightarrow \mathbb{R}^n$ such that $\mathbf{F} = S(\mathbf{Y}, \mathbf{u})$ with \mathbf{Y} distributed according to a reference distribution over \mathbb{R}^m (i.e., standard normal) will result in \mathbf{F} being distributed according to the likelihood conditioned on \mathbf{u} .

1.1 Contributions and outline

This work proposes a novel framework for the use of generative models in inverse problems, which unifies the tasks of simulation (sampling from the likelihood) and inference (sampling from the posterior). Surprisingly, this yields a single invertible mapping $S : \mathbb{R}^{m+n} \rightarrow \mathbb{R}^{m+n}$. This mapping can be learned from training data $\{(\mathbf{u}_i, \mathbf{f}_i)\}_{i=1}^N$ and defines a generative model for simulation and inference in the sense that for given $\mathbf{u} \in \mathbb{R}^n$, $\mathbf{f} \in \mathbb{R}^m$ and \mathbf{X}, \mathbf{Y} distributed according to some reference distribution,

$$(\mathbf{X}', \mathbf{F}) = S(\mathbf{u}, \mathbf{Y}), \quad (\text{simulation})$$

$$(\mathbf{U}, \mathbf{Y}') = S^{-1}(\mathbf{X}, \mathbf{f}), \quad (\text{inference})$$

will yield \mathbf{F} distributed according to the likelihood, conditioned on \mathbf{u} and \mathbf{U} distributed according to the posterior conditioned on \mathbf{f} . Furthermore, \mathbf{X}', \mathbf{Y}' are distributed according to their respective reference distributions. A schematic depiction is shown in figure 1.

We present in this work

- an explicit construction of S in terms of conditional normalising flows (through triangular maps),
- a variational problem to train the map S directly from samples $\{(\mathbf{u}_i, \mathbf{f}_i)\}_{i=1}^N$,
- numerical examples illustrating the potential benefits of this generative framework.

The remainder of the paper is organized as follows. In section 2 we give a brief outline of related approaches. The main results are presented in section 3 and numerical examples are given in section 4. Finally, section 5 concludes the paper.

2 Related work

Closest in spirit to this work is the work by [5] which first proposed to use invertible neural networks for solving inverse problems. Translated to the notation of this paper, they treat the case $m \leq n$ and use an invertible neural network to learn a mapping $S : \mathbb{R}^n \rightarrow \mathbb{R}^{m+k}$ with $k = m - n$. For given data \mathbf{f} and a random sample from latent space \mathbf{x} , this mapping is supposed to produce a sampling from the posterior $\mathbf{u} = S(\mathbf{f}, \mathbf{x})$. This will work in case the underlying likelihood collapses on to the manifold $\mathbf{f} = K\mathbf{u}$ (i.e., noiseless measurements) and will this sample from the prior restricted to this manifold. This approach using generic invertible architectures was later superseded by the use of normalizing flows for amortized Bayesian inference [27, 35, 36, 33], as it provides a more principled way of doing so. This work can be seen as a bridge between these two approaches and provides a unified framework for using invertible mappings for simulation and inference.

Worth mentioning also is the work by [29] which proposes a generic framework for conditioning a given normalizing flow on any of its input variables. In principle, this approach could be applied to use a generic normalizing flow that represents the distribution of (\mathbf{U}, \mathbf{F}) for either simulation (by conditioning on $\mathbf{U} = \mathbf{u}$) or inference (by conditioning on $\mathbf{F} = \mathbf{f}$). Computationally this is expensive though as for each sample a non-linear system of equations needs to be solved. Moreover, the construction is not generic in the sense that the normalizing flow needs to capture the required dependencies. The current work explicitly constructs a mapping that captures these dependencies and allows for sampling of the two conditional distributions more directly. This comes at the cost of having to fix beforehand on which variables one wishes to be able to condition.

We also mention that conditional generative models used to learn undetermined inverse problems reconstructions are widely available in the literature as variants of popular generative models. Examples are conditional normalizing flows [43, 7, 26], conditional diffusion models [8, 37], conditional GANs [28]. Moreover, generative models have been recently used in form of Plug-and-Play models for inverse problems reconstructions [21, 38, 11]. Finally, it is worth mentioning the latest developments in non-deterministic generative models such as stochastic normalising flows [44, 17], stochastic interpolants [3], and diffusion models [40, 8].

3 A generative model for forward and inverse problems

3.1 Notation and preliminaries

Vectors will be denoted by boldface symbols, e.g., $\mathbf{u} \in \mathbb{R}^n, \mathbf{f} \in \mathbb{R}^m$ and operators by italic capitals, e.g., $K : \mathbb{R}^n \rightarrow \mathbb{R}^m$ and $S : \mathbb{R}^{m+n} \rightarrow \mathbb{R}^{m+n}$. Random variables will be denoted by bold capitals, e.g. \mathbf{U}, \mathbf{F} . We denote the probability measure underlying a random variable \mathbf{U} as $\mu_{\mathbf{U}}$. The joint distribution of two variables will be denoted similarly as $\mu_{\mathbf{U}, \mathbf{F}}$. When the distribution is absolutely continuous, we denote the corresponding density as $\pi_{\mathbf{U}}$ etc. For sake of generality, however, and to handle singular data distributions (e.g., data concentrated on manifolds) we will formulate the results preferably in terms of the measures.

The main objects of interest in this paper are the joint distribution $\mu_{\mathbf{U}, \mathbf{F}}$ which describes the relation between \mathbf{U} and \mathbf{F} , its conditionals $\mu_{\mathbf{F}|\mathbf{U}}$ (also referred to as the likelihood) and $\mu_{\mathbf{U}|\mathbf{F}}$ (also referred to as the posterior), and its marginals $\mu_{\mathbf{U}}$ (referred to as the prior in the inverse problems literature) and $\mu_{\mathbf{F}}$. Thanks to the existence of conditional expectations (equivalently by existence of a disintegration) we can write

$$\mu_{\mathbf{U}, \mathbf{F}} = \mu_{\mathbf{F}|\mathbf{U}} \otimes \mu_{\mathbf{U}} = \mu_{\mathbf{U}|\mathbf{F}} \otimes \mu_{\mathbf{F}},$$

where the first equality is intended rigorously as

$$\mathbb{E}_{(\mathbf{u}, \mathbf{f}) \sim \mu_{\mathbf{U}, \mathbf{F}}} \varphi(\mathbf{u}, \mathbf{f}) = \mathbb{E}_{\mathbf{u} \sim \mu_{\mathbf{U}}} \mathbb{E}_{\mathbf{f} \sim \mu_{\mathbf{F}|\mathbf{U}=\mathbf{u}}} \varphi(\mathbf{u}, \mathbf{f})$$

for every test function $\varphi : \mathbb{R}^{m+n} \rightarrow \mathbb{R}$ and the second equality is similarly defined. Note that we denoted by $\mathbb{E}_{\mathbf{w} \sim \mu_{\mathbf{W}}}$ the expectation with respect to a probability measure $\mu_{\mathbf{W}}$. With the goal of ease notation in the proof we will often write $\mathbb{E}_{\mu_{\mathbf{W}}}$ instead of $\mathbb{E}_{\mathbf{w} \sim \mu_{\mathbf{W}}}$. The variable dependence will be clear from the context.

Finally, we denote the push-forward of a measure by the map T by $T_{\#}\mu = \mu \circ T^{-1}$. When applicable, this is denoted in terms of the corresponding density as $T_{\#}\pi = (\pi \circ T^{-1})|\nabla T^{-1}|$. Similarly, the pull-back is denoted as $T^{\#}\mu = \mu \circ T$ and $T^{\#}\pi = (\pi \circ T)|\nabla T|$.

3.2 Conditional sampling using triangular maps

Our starting point is the construction of an invertible mapping F which represents the joint distribution as

$$\mu_{\mathbf{U}, \mathbf{F}} = F_{\#}\mu_{\mathbf{X}, \mathbf{Y}}, \tag{2}$$

with $\mu_{\mathbf{X}, \mathbf{Y}}$ a given reference distribution. Throughout we assume that $\mu_{\mathbf{X}, \mathbf{Y}} = \mu_{\mathbf{X}} \otimes \mu_{\mathbf{Y}}$ and denote by $\mu_{\mathbf{X}}$ and $\mu_{\mathbf{Y}}$ the reference distributions over the latent space, where \mathbf{X} is used to denote the latent variable corresponding to \mathbf{U} , and \mathbf{Y} the latent variable corresponding to \mathbf{F} .

While there are infinitely many maps that will achieve this, triangular maps have the appealing property that they allow for relatively straightforward evaluation of the conditional distributions $\mu_{\mathbf{F}|\mathbf{U}}$ resp. $\mu_{\mathbf{U}|\mathbf{F}}$ when F exhibits lower resp. upper triangular structure. For the sake of completeness we reproduce here the main results required (see e.g., [27, Lemma 1]).

Definition 3.1 (Invertible lower-triangular maps). A map $F : \mathbb{R}^{n+m} \rightarrow \mathbb{R}^{n+m}$ is called lower-triangular if its Jacobian $\nabla F \in \mathbb{R}^{(n+m) \times (n+m)}$ is a lower-triangular matrix. Splitting the variables, it can be expressed as

$$F(\mathbf{x}, \mathbf{y}) = (F_1(\mathbf{x}), F_2(\mathbf{x}, \mathbf{y})),$$

with $F_1 : \mathbb{R}^n \rightarrow \mathbb{R}^n$ and $F_2 : \mathbb{R}^{n+m} \rightarrow \mathbb{R}^m$. We say that F is an invertible lower-triangular map if F is invertible and its inverse $G = F^{-1}$ is lower-triangular, i.e. given by

$$G(\mathbf{u}, \mathbf{f}) = (G_1(\mathbf{u}), G_2(\mathbf{u}, \mathbf{f})).$$

Note that this implies that $G_1 = F_1^{-1}$, and G_2 satisfying

$$G_2(\mathbf{u}, F_2(G_1(\mathbf{u}), \mathbf{y})) = \mathbf{y},$$

and

$$F_2(\mathbf{x}, G_2(F_1(\mathbf{x}), \mathbf{f})) = \mathbf{f}. \quad (3)$$

Definition 3.2 (Invertible upper-triangular maps). A map $F : \mathbb{R}^{n+m} \rightarrow \mathbb{R}^{n+m}$ is called upper-triangular if its Jacobian $\nabla F \in \mathbb{R}^{(n+m) \times (n+m)}$ is an upper-triangular matrix. Splitting the variables, it can be expressed as

$$F(\mathbf{x}, \mathbf{y}) = (F_1(\mathbf{x}, \mathbf{y}), F_2(\mathbf{y})),$$

with $F_1 : \mathbb{R}^{n+m} \rightarrow \mathbb{R}^n$ and $F_2 : \mathbb{R}^m \rightarrow \mathbb{R}^m$. We say that F is an invertible upper-triangular map if F is invertible and its inverse $G = F^{-1}$ is upper-triangular, i.e. given by

$$G(\mathbf{u}, \mathbf{f}) = (G_1(\mathbf{u}, \mathbf{f}), G_2(\mathbf{f})).$$

Note that this implies that $G_2 = F_2^{-1}$, and G_1 satisfying

$$G_1(F_1(\mathbf{x}, G_2(\mathbf{f})), \mathbf{f}) = \mathbf{x},$$

and

$$F_1(G_1(\mathbf{u}, F_2(\mathbf{y})), \mathbf{y}) = \mathbf{u}.$$

The triangular structure of the map F can be exploited to easily condition on either \mathbf{u} or \mathbf{f} , as per the following two lemmas.

Lemma 3.3. *Let $\tilde{F} : \mathbb{R}^{n+m} \rightarrow \mathbb{R}^{n+m}$ be an invertible lower-triangular map satisfying*

$$\tilde{F}_{\#} \mu_{\mathbf{X}, \mathbf{Y}} = \mu_{\mathbf{U}, \mathbf{F}},$$

for a given reference measure $\mu_{\mathbf{X}, \mathbf{Y}}$. Then, for any $\mathbf{u} \in \mathbb{R}^n$, the map

$$F_{\text{like}}(\cdot; \mathbf{u}) := \check{F}_2(\check{F}_1^{-1}(\mathbf{u}), \cdot),$$

with inverse

$$F_{\text{like}}^{-1}(\cdot; \mathbf{u}) := \check{G}_2(\mathbf{u}, \cdot),$$

pushes forward $\mu_{\mathbf{Y}}$ to the conditional measure $\mu_{\mathbf{F}|\mathbf{U}=\mathbf{u}}$, i.e.,

$$\mu_{\mathbf{F}|\mathbf{U}=\mathbf{u}} = F_{\text{like}}(\cdot; \mathbf{u})_{\#} \mu_{\mathbf{Y}}.$$

Proof. We are given that $\mu_{\mathbf{U}, \mathbf{F}} = \check{F}_{\#} \mu_{\mathbf{X}, \mathbf{Y}}$, where \check{F} is invertible and lower-triangular, that is

$$\check{F}(\mathbf{x}, \mathbf{y}) = (\check{F}_1(\mathbf{x}), \check{F}_2(\mathbf{x}, \mathbf{y})).$$

We first prove that $(\check{F}_1)_{\#} \mu_{\mathbf{X}} = \mu_{\mathbf{U}}$. Indeed, by choosing the test function $\varphi(\mathbf{u}, \mathbf{f}) = \psi(\mathbf{u})$ we obtain that

$$\mathbb{E}_{\mu_{\mathbf{U}}} \psi(\mathbf{u}) = \mathbb{E}_{\mu_{(\mathbf{U}, \mathbf{F})}} \varphi(\mathbf{u}, \mathbf{f}) = \mathbb{E}_{\mu_{(\mathbf{X}, \mathbf{Y})}} \psi(\check{F}_1(\mathbf{x})) = \mathbb{E}_{\mu_{\mathbf{X}}} \psi(\check{F}_1(\mathbf{x}))$$

where we used that $\mu_{\mathbf{U}}$ and $\mu_{\mathbf{X}}$ are the marginals of $\pi_{\mathbf{U}, \mathbf{F}}$ and $\pi_{\mathbf{X}, \mathbf{Y}}$ respectively.

Moreover, since \check{F}_1 is invertible, it also holds that $(\check{F}_1^{-1})_{\#} \mu_{\mathbf{U}} = \mu_{\mathbf{X}}$.

By existence of the conditional expectation, we can write $\mu_{\mathbf{U}, \mathbf{F}}$ as

$$\mu_{\mathbf{U}, \mathbf{F}} = \mu_{\mathbf{F}|\mathbf{U}} \otimes \mu_{\mathbf{U}}.$$

To prove that $\mu_{\mathbf{F}|\mathbf{U}=\mathbf{u}} = F_{\text{like}}(\cdot; \mathbf{u})_{\#} \mu_{\mathbf{Y}}$, we will show that the action of $\mu_{\mathbf{F}|\mathbf{U}=\mathbf{u}}$ on test functions matches that of pushing forward $\mu_{\mathbf{Y}}$ through F_{like} . Let $\varphi : \mathbb{R}^m \rightarrow \mathbb{R}$ be any test function. Then

$$\begin{aligned} \mathbb{E}_{\mu_{\mathbf{U}}} \mathbb{E}_{F_{\text{like}}(\cdot; \mathbf{u})_{\#} \mu_{\mathbf{Y}}} \varphi(\mathbf{u}, \mathbf{f}) &= \mathbb{E}_{\mu_{\mathbf{U}}} \mathbb{E}_{\mu_{\mathbf{Y}}} \varphi(\mathbf{u}, F_{\text{like}}(\mathbf{u}, \mathbf{y})) \\ &= \mathbb{E}_{\mu_{\mathbf{U}}} \mathbb{E}_{\mu_{\mathbf{Y}}} \varphi(\mathbf{u}, \check{F}_2(\check{F}_1^{-1}(\mathbf{u}), \mathbf{y})) \\ &= \mathbb{E}_{\mu_{\mathbf{U}}} \mathbb{E}_{\mu_{\mathbf{Y}}} \varphi(\check{F}_1(\check{F}_1^{-1}(\mathbf{u})), \check{F}_2(\check{F}_1^{-1}(\mathbf{u}), \mathbf{y})) \\ &= \mathbb{E}_{\mu_{\mathbf{X}}} \mathbb{E}_{\mu_{\mathbf{Y}}} \varphi(\check{F}_1(\mathbf{x}), \check{F}_2(\mathbf{x}, \mathbf{y})) \\ &= \mathbb{E}_{\mu_{(\mathbf{U}, \mathbf{F})}} \varphi(\mathbf{u}, \mathbf{f}), \end{aligned}$$

where we have used that $(\check{F}_1^{-1})_{\#} \mu_{\mathbf{U}} = \mu_{\mathbf{X}}$, $\mu_{\mathbf{U}, \mathbf{F}} = \check{F}_{\#} \mu_{\mathbf{X}, \mathbf{Y}}$ and the definition of \check{F} . From the previous chain of inequalities and the uniqueness of the conditional expectation it follows that $\mu_{\mathbf{F}|\mathbf{U}=\mathbf{u}} = F_{\text{like}}(\cdot; \mathbf{u})_{\#} \mu_{\mathbf{Y}}$ as we wanted to prove. The definition of $F_{\text{like}}^{-1}(\cdot; \mathbf{u})$ is readily verified by substitution and using the definition of \check{G}_2 (cf. definition 3.1). Indeed, (3) implies that $\check{F}_2(\mathbf{x}, \check{G}_2(\check{F}_1(\mathbf{x}), \mathbf{f})) = \mathbf{f}$ for every \mathbf{x} . Therefore, since the previous relation holds, in particular, for $\mathbf{x} = \check{F}_1^{-1}(\mathbf{u})$ we have

$$F_{\text{like}}(\check{G}_2(\mathbf{u}, \mathbf{f}); \mathbf{u}) = \check{F}_2(\check{F}_1^{-1}(\mathbf{u}), \check{G}_2(\mathbf{u}, \mathbf{f})) = \mathbf{f}$$

as we wanted to prove. \square

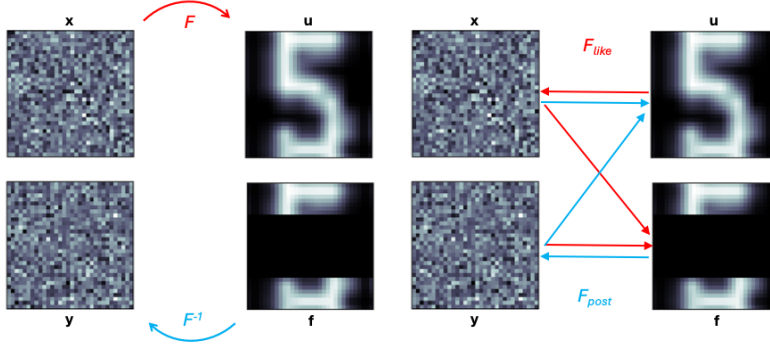


Figure 2: Schematic depiction of the maps F , F_{like} , and F_{post} for an inpainting problem (cf. figure 1). A generic map F will map between (\mathbf{x}, \mathbf{y}) and (\mathbf{u}, \mathbf{f}) (left panel) while the triangular structure allows us to perform conditional sampling $(\mathbf{u}, \mathbf{y}) \mapsto \mathbf{f}$ or $(\mathbf{x}, \mathbf{f}) \mapsto \mathbf{u}$ by either forward or back substitution (right panel).

Lemma 3.4. Let $\hat{F} : \mathbb{R}^{n+m} \rightarrow \mathbb{R}^{n+m}$ be an invertible upper-triangular map satisfying

$$\hat{F}_{\#} \mu_{\mathbf{X}, \mathbf{Y}} = \mu_{\mathbf{U}, \mathbf{F}},$$

for a given reference measure $\mu_{\mathbf{X}, \mathbf{Y}}$. Then, for any $\mathbf{f} \in \mathbb{R}^m$, the map

$$F_{\text{post}}(\cdot; \mathbf{f}) := \hat{F}_1(\cdot, \hat{F}_2^{-1}(\mathbf{f})),$$

with inverse

$$F_{\text{post}}^{-1}(\cdot; \mathbf{f}) := \hat{G}_1(\cdot, \mathbf{f}),$$

pushes forward $\mu_{\mathbf{X}}$ to the conditional measure $\mu_{\mathbf{U}|\mathbf{F}=\mathbf{f}}$, i.e.,

$$\mu_{\mathbf{U}|\mathbf{F}=\mathbf{f}} = F_{\text{post}}(\cdot; \mathbf{f})_{\#} \mu_{\mathbf{X}}.$$

Proof. The proof is similar to that of lemma 3.3. \square

A schematic depiction of the maps F , F_{like} and F_{post} is shown in figure 2.

A practical way to learn a (triangular) map obeying (2) from samples from the joint distribution is by minimizing the KL-divergence

$$\min_F \text{KL}(\mu_{\mathbf{U}, \mathbf{F}}, F_{\#} \mu_{\mathbf{X}, \mathbf{Y}}),$$

which in case $\mu_{\mathbf{X}, \mathbf{Y}}$ is a normal distribution simplifies to

$$\min_F \mathbb{E}_{(\mathbf{u}, \mathbf{f}) \sim \mu_{\mathbf{U}, \mathbf{F}}} \frac{1}{2} \|F^{-1}(\mathbf{u}, \mathbf{f})\|_2^2 - \log |\nabla F^{-1}(\mathbf{u}, \mathbf{f})|.$$

Because of the triangular structure, the problem separates over the components of F and we can train F_{post} and F_{like} directly as per the following lemma.

Lemma 3.5. *The maps F_{post} and F_{like} defined in lemmas 3.4, 3.3 can be obtained by solving the following variational problems*

$$\min_{F_{\text{post}}} \mathbb{E}_{(\mathbf{u}, \mathbf{f}) \sim \mu_{\mathbf{U}, \mathbf{F}}} \frac{1}{2} \|F_{\text{post}}^{-1}(\mathbf{u}; \mathbf{f})\|_2^2 - \log |\nabla F_{\text{post}}^{-1}(\mathbf{u}; \mathbf{f})|.$$

$$\min_{F_{\text{like}}} \mathbb{E}_{(\mathbf{u}, \mathbf{f}) \sim \mu_{\mathbf{U}, \mathbf{F}}} \frac{1}{2} \|F_{\text{like}}^{-1}(\mathbf{f}; \mathbf{u})\|_2^2 - \log |\nabla F_{\text{like}}^{-1}(\mathbf{f}; \mathbf{u})|.$$

Proof. The result follows by plugging in the expressions for the upper and lower triangular maps and identifying the required terms. \square

Remark 3.6. The triangular structure guarantees that the variational problems stated in lemma 3.5 have a unique solution. See for example [25] for an overview of suitable triangular architectures which can be used to parametrize the invertible maps.

3.3 Main results

We now embed the maps F_{post} and F_{like} defined in lemmas 3.4 and 3.3 in a single invertible map $S = (S_1, S_2)$ with inverse $S^{-1} \equiv R = (R_1, R_2)$ as

$$S_1(\mathbf{u}, \mathbf{y}) = F_{\text{post}}^{-1}(\mathbf{u}; F_{\text{like}}(\mathbf{y}; \mathbf{u})), \quad S_2(\mathbf{u}, \mathbf{y}) = F_{\text{like}}(\mathbf{y}; \mathbf{u}), \quad (4)$$

$$R_1(\mathbf{x}, \mathbf{f}) = F_{\text{post}}(\mathbf{x}; \mathbf{f}), \quad R_2(\mathbf{x}, \mathbf{f}) = F_{\text{like}}^{-1}(\mathbf{f}; F_{\text{post}}(\mathbf{x}; \mathbf{f})). \quad (5)$$

By construction we then have

$$S_2(\cdot; \mathbf{u})_{\#} \pi_{\mathbf{Y}} = \mu_{\mathbf{F}|\mathbf{U}=\mathbf{u}},$$

$$R_1(\cdot; \mathbf{f})_{\#} \pi_{\mathbf{X}} = \mu_{\mathbf{U}|\mathbf{F}=\mathbf{f}},$$

such that $\mathbf{f} = S_2(\mathbf{u}, \mathbf{y})$ with $\mathbf{y} \sim \mu_{\mathbf{Y}}$ produces a sample from the likelihood (i.e., a simulation) and $\mathbf{u} = R_1(\mathbf{x}, \mathbf{f})$ with $\mathbf{x} \sim \mu_{\mathbf{X}}$ produces a sample from the posterior (i.e., inference). This map has a number of useful properties, which we outline in the following two theorems.

Theorem 3.7. *Let the maps S and R as defined in (4), (5). Then, it holds that $S^{-1} = R$ and we have*

$$i) (R_1(\cdot, \mathbf{f}))_{\#} \mu_{\mathbf{X}} = \mu_{\mathbf{U}|\mathbf{F}=\mathbf{f}}.$$

$$ii) (S_2(\mathbf{u}, \cdot))_{\#} \mu_{\mathbf{Y}} = \mu_{\mathbf{F}|\mathbf{U}=\mathbf{u}},$$

$$iii) R_{\#} \mu_{\mathbf{X}, \mathbf{F}} = \mu_{\mathbf{U}, \mathbf{Y}},$$

$$iv) S_{\#} \mu_{\mathbf{U}, \mathbf{Y}} = \mu_{\mathbf{X}, \mathbf{F}}.$$

Proof. The relation $S^{-1} = R$ follows from a direct computation, while *i)* and *ii)* hold by construction (cf. lemmas 3.3 and 3.4). We now prove *iii)* and *iv)*. Note

that since $S^{-1} = R$, it is enough to prove *iii*). Given a test function φ , it holds that

$$\begin{aligned}\mathbb{E}_{\mu_{\mathbf{X}, \mathbf{F}}} \varphi(R_1(\mathbf{x}, \mathbf{f}), R_2(\mathbf{x}, \mathbf{f})) &= \mathbb{E}_{\mu_{\mathbf{X}, \mathbf{F}}} \varphi(F_{\text{post}}(\mathbf{x}; \mathbf{f}), F_{\text{like}}^{-1}(\mathbf{f}; F_{\text{post}}(\mathbf{x}; \mathbf{f}))) \\ &= \mathbb{E}_{\mu_{\mathbf{X}, \mathbf{F}}} \varphi(\hat{F}_1(\mathbf{x}, \hat{F}_2^{-1}(\mathbf{f})), F_{\text{like}}^{-1}(\mathbf{f}; \hat{F}_1(\mathbf{x}, \hat{F}_2^{-1}(\mathbf{f})))) \\ &= \mathbb{E}_{\mu_{\mathbf{X}, \mathbf{Y}}} \varphi(\hat{F}_1(\mathbf{x}, \mathbf{y}), F_{\text{like}}^{-1}(\hat{F}_2(\mathbf{y}); \hat{F}_1(\mathbf{x}, \mathbf{y})))\end{aligned}$$

where we used the definition of F_{post} in lemma 3.4 and that $(\hat{F}_2^{-1})_{\#} \mu_{\mathbf{F}} = \mu_{\mathbf{Y}}$. Now, using the definition of F_{like}^{-1} (cf. lemma 3.3) we can continue the previous estimate as

$$\begin{aligned}&= \mathbb{E}_{\mu_{\mathbf{X}, \mathbf{Y}}} \varphi(\hat{F}_1(\mathbf{x}, \mathbf{y}), \check{F}_2^{-1}(\hat{F}_1(\mathbf{x}, \mathbf{y}), \hat{F}_2(\mathbf{y}))) \\ &= \mathbb{E}_{\mu_{\mathbf{U}, \mathbf{F}}} \varphi(\mathbf{u}, \check{G}_2(\mathbf{u}, \mathbf{f})) \\ &= \mathbb{E}_{\mu_{\mathbf{U}, \mathbf{F}}} \varphi(\check{F}_1(\check{F}_1^{-1}(\mathbf{u})), \check{G}_2(\mathbf{u}, \mathbf{f})) \\ &= \mathbb{E}_{\mu_{\mathbf{X}, \mathbf{Y}}} \varphi(\check{F}_1(\mathbf{x}), \mathbf{y}) \\ &= \mathbb{E}_{\mu_{\mathbf{U}, \mathbf{Y}}} \varphi(\mathbf{u}, \mathbf{y})\end{aligned}$$

where additionally we used that $\check{F}_{\#}^{-1} \mu_{\mathbf{U} \times \mathbf{F}} = \mu_{\mathbf{X} \times \mathbf{Y}}$ and that $(\check{F}_1)_{\#} \mu_{\mathbf{X}} = \mu_{\mathbf{U}}$. Because the result holds for arbitrary φ , this proves *iii*). \square

Remark 3.8. Note that *iii*) and *iv*) do not imply *i*) and *ii*) generally. Indeed, if we let $S(\mathbf{u}, \mathbf{y}) = (\check{F}_1(\mathbf{u}), \hat{F}_2(\mathbf{y}))$ we immediately get

$$S^{\#} \mu_{\mathbf{X}, \mathbf{F}} = \mu_{\mathbf{U}, \mathbf{Y}},$$

without achieving the sought representations of the likelihood and posterior. This construction hinges on that fact that $\check{F}_1^{\#} \mu_{\mathbf{X}} = \mu_{\mathbf{U}}$ and $\hat{F}_2^{\#} \mu_{\mathbf{Y}} = \mu_{\mathbf{F}}$. For details see the proof of lemmas 3.3 and 3.4.

A similar (symmetric) result to the one of theorem 3.7 i),ii) can be obtained for the maps R_2 and S_1 .

Theorem 3.9. *Let the maps S and R as defined in (4), (5). Then, it holds that*

- i)* $\mathbb{E}_{\mu_{\mathbf{X}}} [(R_2(\mathbf{x}, \cdot))_{\#} \mu_{\mathbf{F}}] = \mu_{\mathbf{Y}}.$
- ii)* $\mathbb{E}_{\mu_{\mathbf{Y}}} [(S_1(\cdot, \mathbf{y}))_{\#} \mu_{\mathbf{U}}] = \mu_{\mathbf{X}}.$

Proof. We again prove only the statement *i*). Given an arbitrary test function φ

it holds that

$$\begin{aligned}
\mathbb{E}_{\mu_{\mathbf{X}}} \mathbb{E}_{\mu_{\mathbf{F}}} \varphi(R_2(\mathbf{f}, \mathbf{x})) &= \mathbb{E}_{\mu_{\mathbf{X}}} \mathbb{E}_{\mu_{\mathbf{F}}} \varphi(F_{\text{like}}^{-1}(\mathbf{f}; F_{\text{post}}(\mathbf{x}; \mathbf{f}))) \\
&= \mathbb{E}_{\mu_{\mathbf{X}}} \mathbb{E}_{\mu_{\mathbf{F}}} \varphi(F_{\text{like}}^{-1}(\mathbf{f}; \hat{F}_1(\mathbf{x}, \hat{F}_2^{-1}(\mathbf{f}))) \\
&= \mathbb{E}_{\mu_{\mathbf{X}}} \mathbb{E}_{\mu_{\mathbf{F}}} \varphi(\check{F}_2^{-1}(\hat{F}_1(\mathbf{x}, \hat{F}_2^{-1}(\mathbf{f})), \mathbf{f})) \\
&= \mathbb{E}_{\mu_{\mathbf{X}}} \mathbb{E}_{\mu_{\mathbf{Y}}} \varphi(\check{F}_2^{-1}(\hat{F}_1(\mathbf{x}, \mathbf{y}), \hat{F}_2(\mathbf{y}))) \\
&= \mathbb{E}_{\mu_{\mathbf{U}, \mathbf{F}}} \varphi(\check{F}_2^{-1}(\mathbf{u}, \mathbf{f})) \\
&= \mathbb{E}_{\mu_{\mathbf{X}}} \mathbb{E}_{\mu_{\mathbf{Y}}} \varphi(\mathbf{y}) \\
&= \mathbb{E}_{\mu_{\mathbf{Y}}} \varphi(\mathbf{y})
\end{aligned}$$

as we wanted to prove. \square

Remark 3.10. Note that by symmetry (cf. theorem 3.7 i), ii)) we would expect that

$$S_1(\cdot, \mathbf{y})_{\#} \mu_{\mathbf{U}} = \mu_{\mathbf{X}|\mathbf{Y}=\mathbf{y}},$$

and

$$R_2(\mathbf{x}, \cdot)_{\#} \mu_{\mathbf{F}} = \mu_{\mathbf{Y}|\mathbf{X}=\mathbf{x}}.$$

The conditions i), ii) in theorem 3.9 are in fact equivalent since we have assumed $\mu_{\mathbf{X}, \mathbf{Y}} = \mu_{\mathbf{X}} \otimes \mu_{\mathbf{Y}}$.

While we can now construct S explicitly from the two aforementioned triangular maps, we would like to be able to use generic invertible network architectures to represent S . Therefore, we present the following result which entails a training loss that can be evaluated directly on S and S^{-1} .

Corollary 3.11. *Given $S = (S_1, S_2)$ and $R = (R_1, R_2)$ consider the following losses:*

$$\begin{aligned}
\mathcal{J}_1(S) &= \mathcal{M}((I_n, S_2)_{\#} \mu_{\mathbf{U}, \mathbf{Y}}, \mu_{\mathbf{U}, \mathbf{F}}) \\
\mathcal{J}_2(R) &= \mathcal{M}((R_1, I_m)_{\#} \mu_{\mathbf{X}, \mathbf{F}}, \mu_{\mathbf{U}, \mathbf{F}}),
\end{aligned}$$

with

$$(I_n, S_2)(\mathbf{u}, \mathbf{y}) = (\mathbf{u}, S_2(\mathbf{u}, \mathbf{y})), (R_1, I_m)(\mathbf{x}, \mathbf{f}) = (R_1(\mathbf{x}, \mathbf{f}), \mathbf{f}),$$

and where \mathcal{M} is some distance on the space of measures. Then the following statements hold:

- i) $\mathcal{J}_1(S) = 0$ if and only if $(S_2(\mathbf{u}, \cdot))_{\#} \pi_{\mathbf{Y}} = \mu_{\mathbf{F}|\mathbf{U}=\mathbf{u}}$,
- ii) $\mathcal{J}_2(R) = 0$ if and only if $(R_1(\cdot, \mathbf{f}))_{\#} \pi_{\mathbf{X}} = \mu_{\mathbf{U}|\mathbf{F}=\mathbf{f}}$.

Proof. Suppose that $\mathcal{J}_1(S) = 0$. Since \mathcal{M} is a distance on the space of measures it holds that $\mu_{\mathbf{U}} \otimes [(S_2(\mathbf{u}, \cdot))_{\#} \mu_{\mathbf{Y}}] = \mu_{\mathbf{U}, \mathbf{F}}$. Therefore, the relation $(S_2(\mathbf{u}, \cdot))_{\#} \pi_{\mathbf{Y}} = \mu_{\mathbf{F}|\mathbf{U}=\mathbf{u}}$ follows immediately from the uniqueness of conditional expectation. Vice versa, if $(S_2(\mathbf{u}, \cdot))_{\#} \pi_{\mathbf{Y}} = \mu_{\mathbf{F}|\mathbf{U}=\mathbf{u}}$, then, it also holds that $\mu_{\mathbf{U}} \otimes [(S_2(\mathbf{u}, \cdot))_{\#} \mu_{\mathbf{Y}}] = \mu_{\mathbf{U}, \mathbf{F}}$ implying that $\mathcal{J}_1(S) = 0$. The proof of ii) is similar. \square

Remark 3.12. The conditions that $\mathcal{J}_1(S) = \mathcal{J}_2(S^{-1}) = 0$ may not be sufficient to fully constraint the map S . It may therefore be advantageous to add two additional terms:

$$\begin{aligned}\mathcal{J}_3(S) &= \mathcal{M}(S_{\#}\mu_{\mathbf{U}, \mathbf{Y}}, \mu_{\mathbf{X}, \mathbf{F}}), \\ \mathcal{J}_4(R) &= \mathcal{M}(R_{\#}\mu_{\mathbf{X}, \mathbf{F}}, \mu_{\mathbf{U}, \mathbf{Y}}).\end{aligned}$$

If $R = S^{-1}$, then one can observe that some of the conditions given above are redundant.

Theorem 3.13. *Suppose that $R = S^{-1}$. Then*

- i) $\mathcal{J}_3(S) = 0$ if and only if $\mathcal{J}_4(R) = 0$*
- ii) $\mathcal{J}_3(S) = \mathcal{J}_1(S) = 0$ implies $\mathcal{J}_2(R) = 0$*
- iii) $\mathcal{J}_2(R) = \mathcal{J}_4(R) = 0$ implies $\mathcal{J}_1(S) = 0$.*

Proof. Note that *i)* is immediate from the definition of the push-forward and the assumption $R = S^{-1}$. We now prove *ii)* (since proof of *iii)* is similar we omit it). By Corollary 3.11, $\mathcal{J}_1(S) = 0$ implies that $(S_2(\mathbf{u}, \cdot))_{\#}\mu_{\mathbf{Y}} = \mu_{\mathbf{F}|\mathbf{U}=\mathbf{u}}$. Therefore, for every test function φ it holds

$$\begin{aligned}\mathbb{E}_{\mu_{\mathbf{U}, \mathbf{F}}}\varphi(\mathbf{u}, \mathbf{f}) &= \mathbb{E}_{\mu_{\mathbf{U} \times \mathbf{Y}}}\varphi(\mathbf{u}, S_2(\mathbf{y}, \mathbf{u})) = \mathbb{E}_{\mu_{\mathbf{U} \times \mathbf{Y}}}\varphi(R_1(S(\mathbf{y}, \mathbf{u})), S_2(\mathbf{y}, \mathbf{u})) \\ &= \mathbb{E}_{\mu_{\mathbf{F} \times \mathbf{X}}}\varphi(R_1(\mathbf{x}, \mathbf{f}), S_2(R(\mathbf{x}, \mathbf{f}))) \\ &= \mathbb{E}_{\mu_{\mathbf{F} \times \mathbf{X}}}\varphi(R_1(\mathbf{x}, \mathbf{f}), \mathbf{f}) \\ &= \mathbb{E}_{\mu_{\mathbf{F}}}\mathbb{E}_{R_1(\cdot, \mathbf{f})_{\#}\mu_{\mathbf{X}}}\varphi(\mathbf{u}, \mathbf{f})\end{aligned}$$

where in the second equality we used that $R = S^{-1}$ and in the third equality we used that $S_{\#}\pi_{\mathbf{U} \times \mathbf{Y}} = \pi_{\mathbf{F} \times \mathbf{X}}$ that is a consequence of $\mathcal{J}_3(S) = 0$. We thus conclude that $(R_1(\cdot, \mathbf{f}))_{\#}\pi_{\mathbf{X}} = \mu_{\mathbf{U}|\mathbf{F}=\mathbf{f}}$ and therefore $\mathcal{J}_2(R) = 0$. \square

3.4 Practical implementation

For practical implementation we need to find a way to evaluate the losses \mathcal{J}_i without having access to $\mu_{\mathbf{U}, \mathbf{F}}$ explicitly. Natural candidates for the distance \mathcal{M} include the Wasserstein distance, the Maximum Mean Discrepancy and the Sinkhorn loss.

As for architectures, based on the explicit construction outlined in this paper it makes sense to make use of triangular maps to parametrize S as

$$S = U \circ L,$$

with U and L upper and lower triangular maps. Indeed, we see that

$$U(\mathbf{u}, \mathbf{f}) = (F_{\text{post}}(\mathbf{u}; \mathbf{f}), \mathbf{f}), \quad L(\mathbf{u}, \mathbf{y}) = (\mathbf{u}, F_{\text{like}}(\mathbf{y}; \mathbf{u})),$$

yields the desired map. This also indicates a natural parametrization that includes the forward operator:

$$U(\mathbf{u}, \mathbf{f}) = \left(\tilde{U}_1(\mathbf{u}, K^{\top} \mathbf{f}), \tilde{U}_2(\mathbf{f}) \right), \quad L(\mathbf{u}, \mathbf{y}) = \left(\tilde{L}_1(\mathbf{u}), \tilde{L}_2(K\mathbf{u}, \mathbf{y}) \right).$$

Some experimental results using affine maps that include a given forward operator are presented in [42].

Other practical architectures for S include invertible ResNets [9], coupling flows [13, 23], monotone transport maps [27, 31], and neural ODEs [12]. A review of various architectures and their approximation properties is given by [19]. An important aspect of the chosen parametrization is that it should allow for sufficiently rich coupling between \mathbf{u} and \mathbf{f} .

4 Numerical results

4.1 A linear inverse problem with Gaussian distributions

Consider a linear inverse problem with a Gaussian prior $N(\mathbf{0}, \Sigma_{\mathbf{U}})$ and likelihood $N(K\mathbf{u}, \Sigma_{\mathbf{F}})$. The joint density is Gaussian with mean zero and covariance

$$\Sigma_{\mathbf{U}, \mathbf{F}} = \begin{pmatrix} \Sigma_{\mathbf{U}} & \Sigma_{\mathbf{U}} K^{\top} \\ K \Sigma_{\mathbf{U}} & K \Sigma_{\mathbf{U}} K^{\top} + \Sigma_{\mathbf{F}} \end{pmatrix}.$$

The conditional distributions are the likelihood with mean $K\mathbf{u}$ and variance $\Sigma_{\text{like}} = \Sigma_{\mathbf{F}}$ and the posterior with mean $(K^{\top} \Sigma_{\mathbf{F}}^{-1} K + \Sigma_{\mathbf{U}}^{-1})^{-1} K^{\top} \Sigma_{\mathbf{F}}^{-1} \mathbf{f}$ and covariance $\Sigma_{\text{post}} = (K^{\top} \Sigma_{\mathbf{F}}^{-1} K + \Sigma_{\mathbf{U}}^{-1})^{-1}$.

In the case of normalising flows, we look for F such that $\mu_{\mathbf{U}, \mathbf{F}} = F_{\#} \pi_{\mathbf{X}, \mathbf{Y}}$. In this case a linear map suffices and we get the following matrix-representations of the lower and upper triangular maps

$$\begin{aligned} \tilde{F} &= \begin{pmatrix} \Sigma_{\mathbf{U}}^{1/2} & 0 \\ K \Sigma_{\mathbf{U}}^{1/2} & \Sigma_{\mathbf{F}}^{1/2} \end{pmatrix}, \\ \hat{F} &= \begin{pmatrix} \Sigma_{\text{post}}^{1/2} & \Sigma_{\mathbf{U}} K^{\top} (K \Sigma_{\mathbf{U}} K^{\top} + \Sigma_{\mathbf{F}})^{-1/2} \\ 0 & (K \Sigma_{\mathbf{U}} K^{\top} + \Sigma_{\mathbf{F}})^{1/2} \end{pmatrix}, \end{aligned}$$

where $A^{1/2}$ denotes a matrix for which $(A^{1/2})(A^{1/2})^{\top} = A$ and depending on the context is either lower or upper triangular.

The construction proposed in (4) and (5) yields

$$S = \begin{pmatrix} \Sigma_{\text{post}}^{1/2} \Sigma_{\mathbf{U}}^{-1} & -\Sigma_{\text{post}}^{1/2} K^{\top} \Sigma_{\mathbf{F}}^{-1/2} \\ K & \Sigma_{\mathbf{F}}^{1/2} \end{pmatrix}, \quad (6)$$

with inverse

$$R = \begin{pmatrix} \Sigma_{\text{post}}^{1/2} & \Sigma_{\text{post}} K^{\top} \Sigma_{\mathbf{F}}^{-1} \\ -\Sigma_{\mathbf{F}}^{-1/2} K \Sigma_{\text{post}}^{1/2} & \Sigma_{\mathbf{F}}^{1/2} (\Sigma_{\mathbf{F}} + K \Sigma_{\mathbf{U}} K^{\top})^{-1} \end{pmatrix}.$$

It is well-known that the transport maps can be very ill-conditioned, and this is also observed here. We see that conditioning of \tilde{F} for example degenerates when

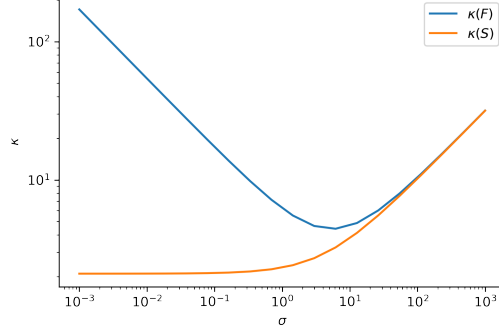


Figure 3: Condition numbers of F and S as a function of the noise level σ .

$\|\Sigma_{\mathbf{F}}\| \rightarrow 0$ (i.e., a deterministic forward model). Note also that the conditioning of \hat{F} is the same, as both are square roots of $\Sigma_{\mathbf{U}, \mathbf{F}}$. The map S on the other hand, does not degenerate as $\|\Sigma_{\mathbf{F}}\| \rightarrow 0$. If $m = n$ and K is invertible, for example, we have

$$S = \begin{pmatrix} 0_{n \times n} & -I_{n \times n} \\ K & 0_{n \times n} \end{pmatrix},$$

and $\kappa(S) = \|K\|_2$. An example is shown in figure 3 for

$$K = \begin{pmatrix} 2 & 1 \\ 1 & 2 \end{pmatrix}, \quad \Sigma_{\mathbf{F}} = \sigma^2 I_{2 \times 2}, \quad \Sigma_{\mathbf{U}} = I_{2 \times 2}.$$

4.2 A non-linear example

We define the target distribution as

$$\mu_{\mathbf{U}, \mathbf{F}} = \check{F}_{\#} \mu_{\mathbf{X}, \mathbf{Y}},$$

with $\mu_{\mathbf{X}, \mathbf{Y}}$ a standard normal distribution over \mathbb{R}^2 and $\check{F} : \mathbb{R}^2 \rightarrow \mathbb{R}^2$ defined as

$$\check{F}(x, y) = \begin{pmatrix} ax \\ \sigma(ax) + by \end{pmatrix}, \quad \check{F}^{-1}(u, f) = \begin{pmatrix} a^{-1}u \\ b^{-1}(f - \sigma(y)) \end{pmatrix},$$

with $a, b > 0$ and $\sigma(\cdot)$ the sign function. The corresponding distributions are visualized in figure 4. In order to construct the map S we fitted an upper triangular map \hat{F} by solving

$$\min_F \mathbb{E}_{(u, f) \sim \mu_{\mathbf{U}, \mathbf{F}}} \frac{1}{2} \|F^{-1}(u, f)\|_2^2 - \log |\nabla F^{-1}(u, f)|,$$

using the **MParT** package [31]. This library parametrizes triangular maps as smooth transformations of multivariate polynomials. For this example we used tensor

products of Hermite polynomials with a total order of 4. The resulting pull-back distribution is depicted in figure 5 while the conditionals are illustrated in figure 6. Using the upper and lower triangular maps \check{F} and \hat{F} , we can now construct S as discussed above. In figure 7 we visualize the flow induced by the maps F and S by plotting the in (at virtual time $t = 0$) and output (at virtual time $t = 1$), connected by a straight line. We see that the lower and upper triangular maps F have a discontinuity at $u = 0$ and $f = 0$ respectively. The condition number of the Jacobian is depicted in figure 8. In this example, the lower triangular map \check{F} is very well-conditioned, at the expense of the upper triangular one \hat{F} being very ill-conditioned. The map S strikes a good balance between these two and has a better conditioning than \hat{F} , though worse than \check{F} .

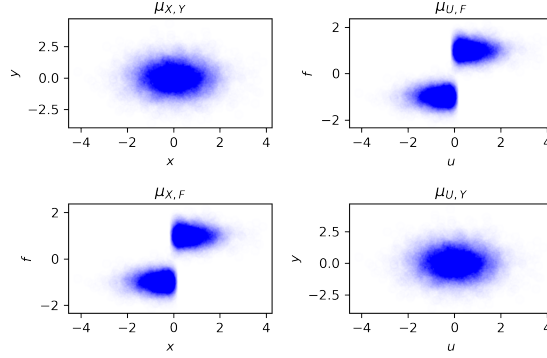


Figure 4: Visualization of the various distributions involved.

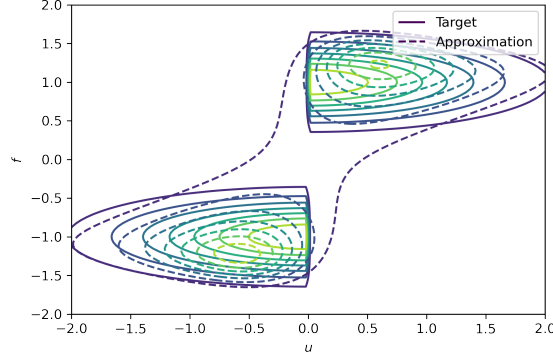


Figure 5: Visualization of $\mu_{U,F}$ and its approximation by $F_{\#}\mu_{X,Y}$

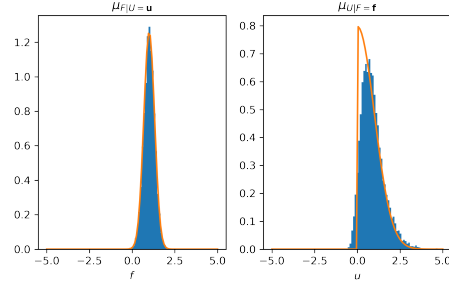


Figure 6: Conditional distributions for $u = 0.5$ and $f = 1$ respectively. The true distribution is depicted in orange, while a histogram of the samples is shown in blue.

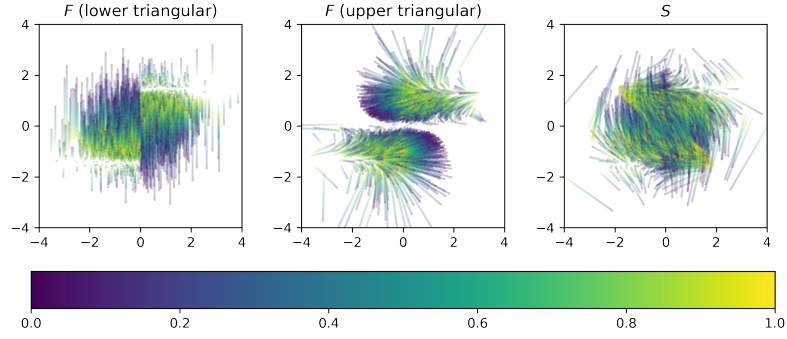


Figure 7: Visualisation of the flows induced by F and S

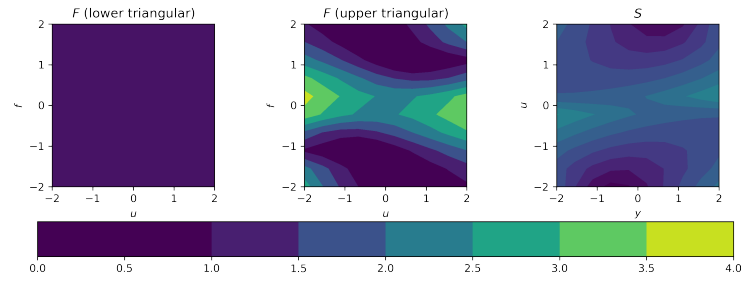


Figure 8: Condition numbers of $\nabla \check{F}$, $\nabla \hat{F}$, and ∇S (on a log scale)

4.3 Inpainting

In this example, we consider an inpainting problem. An example of the training data is shown in figure 9. In order to construct the mapping S , we fit a normal distribution to the training data and construct an affine mapping from this directly, in the same spirit as the example in section 4.1. An example of the result of the mapping applied to the validation data (from the same dataset) is shown in figures 10 and 11. A more detailed look at the generated posterior samples is shown in figure 12.

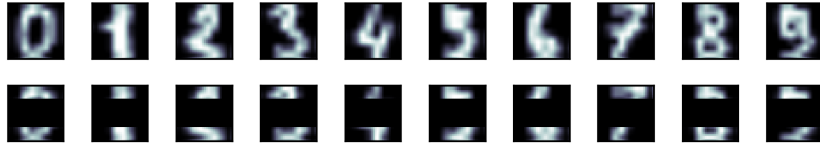


Figure 9: Example of the training data, consisting of handwritten digits from the MNIST dataset (top) and their partially obscured version (bottom).

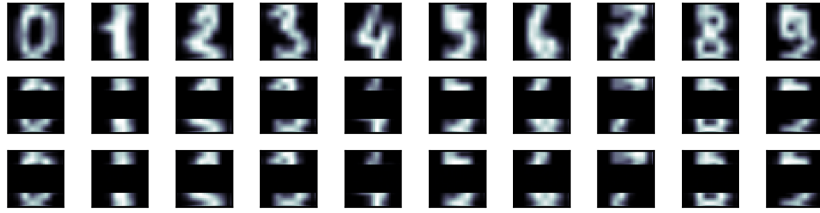


Figure 10: Example of the output of S in simulation mode. The top row shows the input images \mathbf{u} while the middle row shows the corresponding true measurements \mathbf{f} . The bottom row shows the output of S , showing a good match to the expected output.

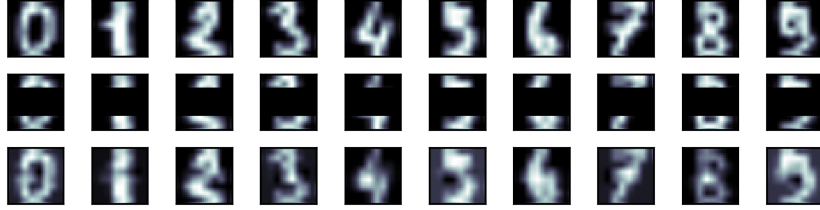


Figure 11: Example of the output of S in inference mode. The top row shows the input images \mathbf{u} while the middle row shows the corresponding true measurements \mathbf{f} . The bottom row shows the output of S^{-1} , showing a good match to the expected output.

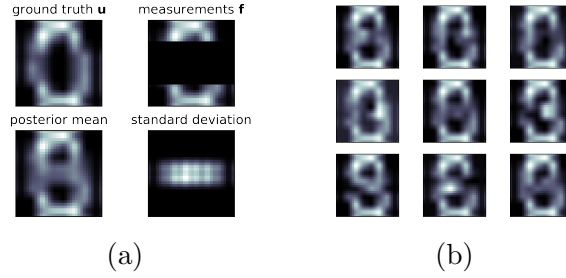


Figure 12: Example of the output of S in inference mode. Left we see true digit ('0') and the corresponding measurement. The posterior mean and pixel-wise standard deviation are shown next to it, indicating the expected uncertainty regarding the inpainted result. On the right, we see a number of samples from the posterior, indicating plausible inpainted results, which include digits resembling an 0, 3, 8, and 9, as expected.

5 Conclusion and discussion

We presented a generic framework for simulation and inference using invertible mappings. The proposed construction has the unique feature that simulation and inference can be performed with a single generative model, run in either forward or reverse mode. Possible advantages of the proposed construction include the improved conditioning of the mapping that needs to be learned, and the fact that only a single mapping needs to be learned. While the current work focuses on the construction of the mapping using deterministic generative models (normalizing flows, invertible neural networks, neural ODEs) we see opportunities to extend it to non-deterministic generative models such as stochastic interpolants and diffusion models. We also aim to explore the use of this framework for experiments design by introducing an additional design parameter, \mathbf{s} , over which the model will be amortized in the training stage. The resulting mapping $S(\mathbf{s}) : \mathbb{R}^{m+n} \rightarrow \mathbb{R}^{m+n}$ is invertible for every \mathbf{s} and can be used for simulation and inference, and hence for experimental design.

References

- [1] Jonas Adler and Ozan Öktem. Deep bayesian inversion. *arXiv preprint arXiv:1811.05910*, 2018.
- [2] Jonas Adler and Ozan Öktem. Learned primal-dual reconstruction. *IEEE transactions on medical imaging*, 37(6):1322–1332, 2018.
- [3] Michael S Albergo, Nicholas M Boffi, and Eric Vanden-Eijnden. Stochastic interpolants: A unifying framework for flows and diffusions. *arXiv preprint arXiv:2303.08797*, 2023.
- [4] Nick Alger, Tucker Hartland, Noemi Petra, and Omar Ghattas. Point spread function approximation of high-rank hessians with locally supported nonnegative integral kernels. *SIAM Journal on Scientific Computing*, 46(3):A1658–A1689, 2024.
- [5] Lynton Ardizzone, Jakob Kruse, Sebastian J Wirkert, Daniel Rahner, Eric W Pellegrini, Ralf S Klessen, Lena Maier-Hein, Carsten Rother, and Ullrich Köthe. Analyzing inverse problems with invertible neural networks. *CoRR*, 2018.
- [6] Simon Arridge, Peter Maass, Ozan Öktem, and Carola-Bibiane Schönlieb. Solving inverse problems using data-driven models. *Acta Numerica*, 28:1–174, 2019.
- [7] Georgios Batzolis, Marcello Carioni, Christian Etmann, Soroosh Afyouni, Zoe Kourtzi, and Carola-Bibiane Schönlieb. CAFLOW: Conditional autoregressive flows. *Foundations of Data Science*, 6(4):553–583, 2024.
- [8] Georgios Batzolis, Jan Stanczuk, Carola-Bibiane Schönlieb, and Christian Etmann. Conditional image generation with score-based diffusion models. *arXiv preprint arXiv:2111.13606*, 2021.
- [9] Jens Behrmann, Will Grathwohl, Ricky TQ Chen, David Duvenaud, and Jörn-Henrik Jacobsen. Invertible residual networks. In *International conference on machine learning*, pages 573–582. PMLR, 2019.
- [10] Nicolas Brosse, Alain Durmus, and Eric Moulines. The promises and pitfalls of stochastic gradient langevin dynamics. In S. Bengio, H. Wallach, H. Larochelle, K. Grauman, N. Cesa-Bianchi, and R. Garnett, editors, *Advances in Neural Information Processing Systems*, volume 31. Curran Associates, Inc., 2018.
- [11] Marcello Carioni, Subhadip Mukherjee, Hong Ye Tan, and Junqi Tang. Unsupervised approaches based on optimal transport and convex analysis for inverse problems in imaging. In *Data-driven Models in Inverse Problems*. Walter de Gruyter GmbH & Co. KG, 2024.
- [12] Ricky T. Q. Chen, Yulia Rubanova, Jesse Bettencourt, and David K Duvenaud. Neural ordinary differential equations. In S. Bengio, H. Wallach, H. Larochelle, K. Grauman, N. Cesa-Bianchi, and R. Garnett, editors, *Advances in Neural Information Processing Systems*, volume 31. Curran Associates, Inc., 2018.

- [13] Laurent Dinh, Jascha Sohl-Dickstein, and Samy Bengio. Density estimation using real NVP. In *International Conference on Learning Representations*, 2017.
- [14] Davis Gilton, Gregory Ongie, and Rebecca Willett. Deep equilibrium architectures for inverse problems in imaging. *IEEE Transactions on Computational Imaging*, 7:1123–1133, 2021.
- [15] Ian Goodfellow, Jean Pouget-Abadie, Mehdi Mirza, Bing Xu, David Warde-Farley, Sherjil Ozair, Aaron Courville, and Yoshua Bengio. Generative adversarial networks. *Communications of the ACM*, 63(11):139–144, 2020.
- [16] Bahadır Gunturk and Xin Li. *Image restoration*. CRC Press, 2018.
- [17] Paul Hagemann, Johannes Hertrich, and Gabriele Steidl. Stochastic normalizing flows for inverse problems: A markov chains viewpoint. *SIAM/ASA Journal on Uncertainty Quantification*, 10(3):1162–1190, 2022.
- [18] Per Christian Hansen, Jakob Jørgensen, and William RB Lionheart. *Computed tomography: algorithms, insight, and just enough theory*. SIAM, 2021.
- [19] Isao Ishikawa, Takeshi Teshima, Koichi Tojo, Kenta Oono, Masahiro Ikeda, and Masashi Sugiyama. Universal approximation property of invertible neural networks. *Journal of Machine Learning Research*, 24(287):1–68, 2023.
- [20] Kyong Hwan Jin, Michael T McCann, Emmanuel Froustey, and Michael Unser. Deep convolutional neural network for inverse problems in imaging. *IEEE transactions on image processing*, 26(9):4509–4522, 2017.
- [21] Ulugbek S Kamilov, Hassan Mansour, and Brendt Wohlberg. A plug-and-play priors approach for solving nonlinear imaging inverse problems. *IEEE Signal Processing Letters*, 24(12):1872–1876, 2017.
- [22] Diederik P Kingma and Max Welling. Auto-encoding variational bayes. *arXiv preprint arXiv:1312.6114*, 2013.
- [23] Durk P Kingma and Prafulla Dhariwal. Glow: Generative flow with invertible 1x1 convolutions. In S. Bengio, H. Wallach, H. Larochelle, K. Grauman, N. Cesa-Bianchi, and R. Garnett, editors, *Advances in Neural Information Processing Systems*, volume 31. Curran Associates, Inc., 2018.
- [24] Durk P Kingma, Tim Salimans, Rafal Jozefowicz, Xi Chen, Ilya Sutskever, and Max Welling. Improved variational inference with inverse autoregressive flow. *Advances in neural information processing systems*, 29, 2016.
- [25] Ivan Kobyzev, Simon J.D. Prince, and Marcus A. Brubaker. Normalizing Flows: An Introduction and Review of Current Methods. *IEEE Transactions on Pattern Analysis and Machine Intelligence*, 43(11):3964–3979, 2021.
- [26] Andreas Lugmayr, Martin Danelljan, Luc Van Gool, and Radu Timofte. Sr-flow: Learning the super-resolution space with normalizing flow. In *European conference on computer vision*, pages 715–732. Springer, 2020.
- [27] Youssef Marzouk, Tarek Moselhy, Matthew Parno, and Alessio Spantini. Sampling via measure transport: An introduction. *Handbook of Uncertainty Quantification*, pages 785–825, 2017.

- [28] Mehdi Mirza and Simon Osindero. Conditional generative adversarial nets. *arXiv preprint arXiv:1411.1784*, 2014.
- [29] Vincent Moens, Aivar Sootla, Haitham Bou Ammar, and Jun Wang. VISCOS flows: Variational schur conditional sampling with normalizing flows, 2022.
- [30] Vishal Monga, Yuelong Li, and Yonina C Eldar. Algorithm unrolling: Interpretable, efficient deep learning for signal and image processing. *IEEE Signal Processing Magazine*, 38(2):18–44, 2021.
- [31] MParT Development Team. Monotone Parameterization Toolkit (MParT), 2022. Version 1.0.0.
- [32] Subhadip Mukherjee, Marcello Carioni, Ozan Öktem, and Carola-Bibiane Schönlieb. End-to-end reconstruction meets data-driven regularization for inverse problems. *Advances in Neural Information Processing Systems*, 34:21413–21425, 2021.
- [33] Rafael Orozco, Ali Siahkoohi, Mathias Louboutin, and Felix J Herrmann. Aspire: iterative amortized posterior inference for bayesian inverse problems. *Inverse Problems*, 41(4):045001, 2025.
- [34] Giorgio Patrini, Rianne Van den Berg, Patrick Forre, Marcello Carioni, Samarth Bhargav, Max Welling, Tim Genewein, and Frank Nielsen. Sinkhorn autoencoders. In *Uncertainty in Artificial Intelligence*, pages 733–743. PMLR, 2020.
- [35] Stefan T. Radev, Ulf K. Mertens, Andreas Voss, Lynton Ardizzone, and Ullrich Kothe. BayesFlow: learning complex stochastic models with invertible neural networks. *IEEE Transactions on Neural Networks and Learning Systems*, 33(4):1452–1466, April 2022.
- [36] Stefan T. Radev, Marvin Schmitt, Valentin Pratz, Umberto Picchini, Ullrich Köthe, and Paul-Christian Bürkner. Jana: jointly amortized neural approximation of complex bayesian models. In *Proceedings of the Thirty-ninth Conference on Uncertainty in Artificial Intelligence*, pages 1695–1706. PMLR, July 2023. ISSN: 2640-3498.
- [37] Kashif Rasul, Calvin Seward, Ingmar Schuster, and Roland Vollgraf. Autoregressive denoising diffusion models for multivariate probabilistic time series forecasting. In *International conference on machine learning*, pages 8857–8868. PMLR, 2021.
- [38] Yaniv Romano, Michael Elad, and Peyman Milanfar. The little engine that could: Regularization by denoising (red). *SIAM journal on imaging sciences*, 10(4):1804–1844, 2017.
- [39] Otmar Scherzer, Markus Grasmair, Harald Grossauer, Markus Haltmeier, and Frank Lenzen. *Variational methods in imaging*, volume 167. Springer, 2009.
- [40] Yang Song, Jascha Sohl-Dickstein, Diederik P Kingma, Abhishek Kumar, Stefano Ermon, and Ben Poole. Score-based generative modeling through stochastic differential equations. *arXiv preprint arXiv:2011.13456*, 2020.

- [41] Albert Tarantola. *Inverse Problem Theory and Methods for Model Parameter Estimation*. Society for Industrial and Applied Mathematics, 2005.
- [42] Tristan van Leeuwen. The reversible simulator – a data-driven approach for solving forward and inverse problems. In *Applications of Mathematics in Sciences, Engineering, and Economics*, Springer Proceedings in Mathematics & Statistics, 2025.
- [43] Christina Winkler, Daniel Worrall, Emiel Hoogetboom, and Max Welling. Learning likelihoods with conditional normalizing flows. *arXiv preprint arXiv:1912.00042*, 2019.
- [44] Hao Wu, Jonas Köhler, and Frank Noé. Stochastic normalizing flows. *Advances in neural information processing systems*, 33:5933–5944, 2020.
- [45] Bo Zhu, Jeremiah Z Liu, Stephen F Cauley, Bruce R Rosen, and Matthew S Rosen. Image reconstruction by domain-transform manifold learning. *Nature*, 555(7697):487–492, 2018.